Dielectric response theory for electron energy loss in clad cylindrical systems

Y. H. Tu and C. M. Kwei
Department of Electronics Engineering, National Chiao Tung University, Hsinchu 300, Taiwan

Y. C. Li
Device Simulation and Modeling Department, Device Division, ProMOS Technologies Inc., Hsinchu 300, Taiwan

C. J. Tung
Department of Nuclear Science, National Tsing Hua University, Hsinchu 300, Taiwan
(Received 10 January 2006; revised manuscript received 26 May 2006; published 6 July 2006)

Inelastic interactions between an electron and a clad cylindrical system were investigated using the dielectric response theory. By solving the Poisson equation and applying the boundary conditions, these interactions were formulated in terms of the surface, interface and volume excitations. Formulas of the differential inverse inelastic mean free path (DIIMFP) were derived for electrons moving parallel to the axis of such a cylindrical structure. A sum-rule-constrained extended Drude dielectric function with spatial dispersion was applied to the calculations of the DIIMFP for a Si cylindrical tube or a Si cylinder clad in a SiO_2 film. For the Si tube, it was found that surface excitations occurred as electrons moved near either the inner or outer surface of the tube and either inside or outside Si. Whereas, volume excitations arose only for electrons moving inside Si. Surface excitations increased, or volume excitations decreased, as electrons moved closer to the surface. For the Si cylinder clad in the SiO_2 film, inelastic interactions were contributed from volume, surface, and interface excitations. Calculated results showed that the relative importance of these excitations depended on the electron distance from the surface or interface of the cylindrical system, the radius of the Si cylinder, and the thickness of the SiO_2 film.

DOI: 10.1103/PhysRevB.74.045403 PACS number(s): 73.22.−f, 78.20.Bh, 78.70.−g

I. INTRODUCTION

In the past few years, new developments in fabrications have allowed the production of miniaturized devices with typical sizes ranging in the nanometer scale. The study of these devices in surface sensitive electron spectroscopies has become an active field of research. Quantitative information on the electron inelastic interaction cross sections plays a crucial role in such surface spectroscopies.[1–6] Several theoretical approaches have been developed to evaluate these cross sections in cylindrical wires and cavities.[7–14] Clad cylindrical systems have also attracted some attention. Expressions of inelastic cross section for electrons in such systems[15,16] were derived based on the frequency dependent dielectric function, i.e., neglecting spatial dispersion. The inclusion of spatial dispersion may be important at short distances from the surface and the interface, where electrons might couple to short-wavelength modes.[17]

In surface sensitive electron spectroscopies, electron inelastic cross sections comprise mainly the contributions from volume, surface, and interface excitations. These excitations can be described based on the dielectric approaches.[18,19] In the present work, a general expression for the differential inverse inelastic mean free path (DIIMFP) was derived for electrons moving parallel to the axis of an infinitely long clad cylindrical system. The sum-rule-constrained extended Drude dielectric function with spatial dispersion,[20] which was successively applied in the calculations of electron inelastic interaction cross sections in a semi-infinite[21,22] and an overlayer system,[23,24] was used to calculate the DIIMFP in this clad cylindrical system. The present calculations were made for electrons moving parallel to the axis of either a Si cylindrical tube or a Si cylinder clad in a SiO_2 film. The dependences of the DIIMFP on the electron position and energy were analyzed. Note that all quantities in this paper are expressed in atomic units (a.u.) unless otherwise specified.

II. THEORY

Figure 1 illustrates the studied problem. An electron with velocity $\vec{v}$ moves parallel to the axis of two infinitely long, coaxial cylindrical interfaces of inner radius a and outer radius b. The cylinder has dielectric functions $\varepsilon_1(k,\omega)$, $\varepsilon_2(k,\omega)$, and $\varepsilon_3(k,\omega)$ in different radii ρ for $\rho<a$, $a<\rho<b$, and $\rho>b$, respectively. At time t, the electron is at a position $\vec{x}_0=(\rho_0,0,vt)$ in cylindrical coordinates.

In the present work, we consider three different cases, i.e., $\rho_0<a$ (case I), $a<\rho_0<b$ (case II), and $\rho_0>b$ (case III). For the sake of simplicity, we consider only the component parallel to the trajectory in the spatial dispersion. Thus, the Fourier transforms of the potentials are (Ref. 25)

$$\Phi_1^{(p)}(\rho,\phi,k,\omega)=\frac{-4\pi}{\varepsilon_1(k,\omega)}\sum_{m=-\infty}^{\infty}A_m^{(p)}(k,\omega)I_m(k\rho)e^{im\phi}\delta(\omega-kv)+\delta_{p,1}\frac{1}{\varepsilon_1(k,\omega)}\Phi_0(\rho,\phi,k,\omega) \quad (1a)$$

for $\rho<a$,

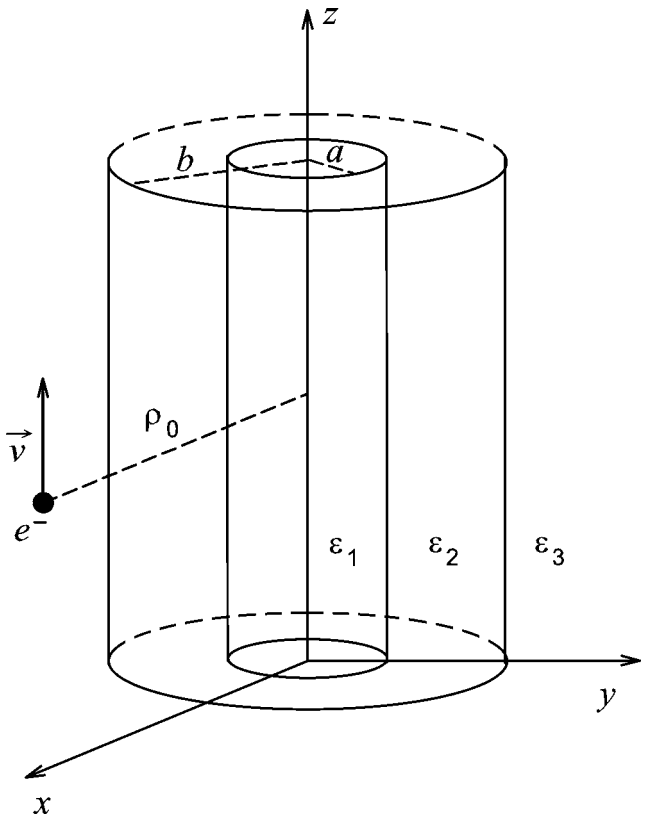

FIG. 1. A sketch of the problem studied in the present work. An electron of velocity $\vec{v}$ moves parallel to and at a distance ρ_0 from the axis of an infinitely long clad cylindrical system with inner radius a and outer radius b. The media in the regions $\rho<a$, $a<\rho<b$, and $\rho>b$ have dielectric functions $\varepsilon_1(k,\omega)$, $\varepsilon_2(k,\omega)$, and $\varepsilon_3(k,\omega)$, respectively.

$$\Phi_2^{(p)}(\rho,\phi,k,\omega)=\frac{-4\pi}{\varepsilon_2(k,\omega)}\sum_{m=-\infty}^{\infty}[B_m^{(p)}(k,\omega)I_m(k\rho)+C_m^{(p)}(k,\omega)K_m(k\rho)]e^{im\phi}\delta(\omega-k\nu)+\delta_{p,\mathrm{II}}\frac{1}{\varepsilon_2(k,\omega)}\Phi_0(\rho,\phi,k,\omega) \tag{1b}$$

for $a<\rho<b$, and

$$\Phi_3^{(p)}(\rho,\phi,k,\omega)=\frac{-4\pi}{\varepsilon_3(k,\omega)}\sum_{m=-\infty}^{\infty}D_m^{(p)}(k,\omega)K_m(k\rho)e^{im\phi}\delta(\omega-k\nu)+\delta_{p,\mathrm{III}}\frac{1}{\varepsilon_3(k,\omega)}\Phi_0(\rho,\phi,k,\omega) \tag{1c}$$

for $\rho>b$. Here $A_m^{(p)}$, $B_m^{(p)}$, $C_m^{(p)}$, and $D_m^{(p)}$ are coefficients to be determined, p=I, II, and III are for cases I, II, and III, respectively, I_m and K_m are modified Bessel functions, δ is the delta function,

$$\Phi_0(\rho,\phi,k,\omega)=-4\pi\sum_{m=-\infty}^{\infty}I_m(k\rho_<)K_m(k\rho_>)e^{im\phi}\delta(\omega-k\nu) \tag{2}$$

is the potential of the electron in vacuum with $\rho_>=\max(\rho,\rho_0)$ and $\rho_<=\min(\rho,\rho_0)$.

A. Case I. Electrons moving in medium 1 (i.e., $\rho_0<a$)

By matching the boundary conditions, i.e., continuities of the potential and the normal component of electric displacement at the interfaces $\rho=a$ and $\rho=b$, one finds

$$A_m^{(\mathrm{I})}(k,\omega)=B_m^{(\mathrm{I})}(k,\omega)+[C_m^{(\mathrm{I})}(k,\omega)-I_m(k\rho_0)]\frac{K_m'(ka)}{I_m'(ka)}, \tag{3a}$$

$$B_m^{(\mathrm{I})}(k,\omega)=\frac{[\varepsilon_3(k,\omega)-\varepsilon_2(k,\omega)]C_m^{(\mathrm{I})}(k,\omega)}{\varepsilon_2(k,\omega)\dfrac{I_m'(kb)}{K_m'(kb)}-\varepsilon_3(k,\omega)\dfrac{I_m(kb)}{K_m(kb)}}, \tag{3b}$$

$$C_m^{(\mathrm{I})}(k,\omega)=\frac{\varepsilon_2(k,\omega)\left[\dfrac{K_m'(ka)}{I_m'(ka)}-\dfrac{K_m(ka)}{I_m(ka)}\right]I_m(k\rho_0)}{\dfrac{[\varepsilon_3(k,\omega)-\varepsilon_2(k,\omega)][\varepsilon_2(k,\omega)-\varepsilon_1(k,\omega)]}{\varepsilon_2(k,\omega)\dfrac{I_m'(kb)}{K_m'(kb)}-\varepsilon_3(k,\omega)\dfrac{I_m(kb)}{K_m(kb)}}+\varepsilon_2(k,\omega)\dfrac{K_m'(ka)}{I_m'(ka)}-\varepsilon_1(k,\omega)\dfrac{K_m(ka)}{I_m(ka)}}, \tag{3c}$$

$$D_m^{(\mathrm{I})}(k,\omega)=\frac{I_m'(kb)}{K_m'(kb)}B_m^{(\mathrm{I})}(k,\omega)+C_m^{(\mathrm{I})}(k,\omega), \tag{3d}$$

where $I_m'(x)=dI_m(x)/dx$ and $K_m'(x)=dK_m(x)/dx$. Removing the vacuum potential and taking the inverse Fourier transform, one obtains the induced potential in the spatial space as follows:

$$\Phi_{1,ind}^{(\mathrm{I})}(\rho,\phi,z,t)=\frac{-2}{\pi v}\sum_{m=-\infty}^{\infty}e^{im\phi}\int_0^E d\omega\left[I_m\left(\frac{\omega}{v}\rho\right)\left\{\mathrm{Re}\left[\frac{A_m^{(\mathrm{I})}\left(\frac{\omega}{v},\omega\right)}{\varepsilon_1\left(\frac{\omega}{v},\omega\right)}\right]\cos\left(\omega\left(\frac{z}{v}-t\right)\right)-\mathrm{Im}\left[\frac{A_m^{(\mathrm{I})}\left(\frac{\omega}{v},\omega\right)}{\varepsilon_1\left(\frac{\omega}{v},\omega\right)}\right]\sin\left(\omega\left(\frac{z}{v}-t\right)\right)\right\}\right.$$
$$\left.+I_m\left(\frac{\omega}{v}\rho_<\right)K_m\left(\frac{\omega}{v}\rho_>\right)\left\{\mathrm{Re}\left[\frac{1}{\varepsilon_1\left(\frac{\omega}{v},\omega\right)}-1\right]\cos\left(\omega\left(\frac{z}{v}-t\right)\right)-\mathrm{Im}\left[\frac{1}{\varepsilon_1\left(\frac{\omega}{v},\omega\right)}\right]\sin\left(\omega\left(\frac{z}{v}-t\right)\right)\right\}\right], \tag{4}$$

where $E=v^2/2$. Note that the upper limit of integration is the maximum energy transfer available.[26] The stopping power, $F^{(\mathrm{I})}$, is related to the derivative of $\Phi_{1,ind}^{(\mathrm{I})}(\rho,\phi,z,t)$ at the position of electrons. One gets

$$F^{(\mathrm{I})}=\frac{-2}{\pi v^2}\sum_{m=-\infty}^{\infty}\int_0^E d\omega\omega I_m\left(\frac{\omega}{v}\rho_0\right)\left\{\mathrm{Im}\left[\frac{A_m{}^{(\mathrm{I})}\left(\frac{\omega}{v},\omega\right)}{\varepsilon_1\left(\frac{\omega}{v},\omega\right)}\right]\right.$$
$$\left.+K_m\left(\frac{\omega}{v}\rho_0\right)\mathrm{Im}\left[\frac{1}{\varepsilon_1\left(\frac{\omega}{v},\omega\right)}\right]\right\}. \tag{5}$$

Thus, the DIIMFP is given by

$$\mu^{(\mathrm{I})}(E,\omega)=\frac{-2}{\pi\nu^2}\sum_{m=-\infty}^{\infty}I_m\left(\frac{\omega}{\nu}\rho_0\right)\left\{\mathrm{Im}\left[\frac{A_m{}^{(\mathrm{I})}\left(\frac{\omega}{\nu},\omega\right)}{\varepsilon_1\left(\frac{\omega}{\nu},\omega\right)}\right]\right.$$
$$\left.+K_m\left(\frac{\omega}{\nu}\rho_0\right)\mathrm{Im}\left[\frac{1}{\varepsilon_1\left(\frac{\omega}{\nu},\omega\right)}\right]\right\}. \tag{6}$$

B. Case II. Electrons moving in medium 2 (i.e., $a<\rho_0<b$)

A similar approach can be made for electrons moving in medium 2. After some mathematical manipulations, one finds

$$A_m^{(\mathrm{II})}(k,\omega)=B_m^{(\mathrm{II})}(k,\omega)+\frac{K_m'(ka)}{I_m'(ka)}C_m{}^{(\mathrm{II})}(k,\omega)+K_m(k\rho_0), \tag{7a}$$

$$B_m^{(\mathrm{II})}(k,\omega)=\frac{[\varepsilon_3(k,\omega)-\varepsilon_2(k,\omega)]\{X_m(k,\omega)I_m(k\rho_0)-[\varepsilon_2(k,\omega)-\varepsilon_1(k,\omega)]K_m(k\rho_0)\}}{X_m(k,\omega)Y_m(k,\omega)-[\varepsilon_2(k,\omega)-\varepsilon_3(k,\omega)][\varepsilon_2(k,\omega)-\varepsilon_1(k,\omega)]}, \tag{7b}$$

$$C_m^{(\mathrm{II})}(k,\omega)=\frac{[\varepsilon_1(k,\omega)-\varepsilon_2(k,\omega)]\{Y_m(k,\omega)K_m(k\rho_0)-[\varepsilon_2(k,\omega)-\varepsilon_3(k,\omega)]I_m(k\rho_0)\}}{X_m(k,\omega)Y_m(k,\omega)-[\varepsilon_2(k,\omega)-\varepsilon_1(k,\omega)][\varepsilon_2(k,\omega)-\varepsilon_3(k,\omega)]}, \tag{7c}$$

$$D_m{}^{(\mathrm{II})}(k,\omega)=\frac{I_m{}'(kb)}{K_m{}'(kb)}B_m{}^{(\mathrm{II})}(k,\omega)+C_m{}^{(\mathrm{II})}(k,\omega)+I_m(k\rho_0), \tag{7d}$$

where

$$X_m(k,\omega)=\varepsilon_2(k,\omega)\frac{K_m{}'(ka)}{I_m{}'(ka)}-\varepsilon_1(k,\omega)\frac{K_m(ka)}{I_m(ka)} \tag{8a}$$

and

$$Y_m(k,\omega) = \varepsilon_2(k,\omega)\frac{I_m{}'(kb)}{K_m{}'(kb)} - \varepsilon_3(k,\omega)\frac{I_m(kb)}{K_m(kb)}. \tag{8b}$$

The DIIMFP is given by

$$\mu^{(\mathrm{II})}(E,\omega) = \frac{-2}{\pi\nu^2}\sum_{m=-\infty}^{\infty}\left\{ I_m\left(\frac{\omega}{\nu}\rho_0\right)\mathrm{Im}\left[\frac{B_m{}^{(\mathrm{II})}\left(\frac{\omega}{\nu},\omega\right)}{\varepsilon_2\left(\frac{\omega}{\nu},\omega\right)}\right] + K_m\left(\frac{\omega}{\nu}\rho_0\right)\mathrm{Im}\left[\frac{C_m{}^{(\mathrm{II})}\left(\frac{\omega}{\nu},\omega\right)}{\varepsilon_2\left(\frac{\omega}{\nu},\omega\right)}\right] + I_m\left(\frac{\omega}{\nu}\rho_0\right)K_m\left(\frac{\omega}{\nu}\rho_0\right)\mathrm{Im}\left[\frac{1}{\varepsilon_2\left(\frac{\omega}{\nu},\omega\right)}\right]\right\}. \tag{9}$$

C. Case III. Electrons moving in medium 3 (i.e., $\rho_0 > b$)

Again, a similar approach can be made for electrons moving in medium 3. After mathematical manipulations, the coefficients can be found as follows:

$$A_m^{(\mathrm{III})}(k,\omega) = B_m{}^{(\mathrm{III})}(k,\omega) + \frac{K_m'(ka)}{I_m'(ka)}C_m{}^{(\mathrm{III})}(k,\omega), \tag{10a}$$

$$B_m^{(\mathrm{III})}(k,\omega) = \frac{\varepsilon_2(k,\omega)\left[\frac{I_m'(kb)}{K_m'(kb)} - \frac{I_m(kb)}{K_m(kb)}\right]K_m(k\rho_0)}{\frac{[\varepsilon_1(k,\omega)-\varepsilon_2(k,\omega)][\varepsilon_2(k,\omega)-\varepsilon_3(k,\omega)]}{\varepsilon_2(k,\omega)\frac{K_m'(ka)}{I_m'(ka)} - \varepsilon_1(k,\omega)\frac{K_m(ka)}{I_m(ka)}} + \varepsilon_2(k,\omega)\frac{I_m'(kb)}{K_m'(kb)} - \varepsilon_3(k,\omega)\frac{I_m(kb)}{K_m(kb)}}, \tag{10b}$$

$$C_m^{(\mathrm{III})}(k,\omega) = \frac{[\varepsilon_1(k,\omega)-\varepsilon_2(k,\omega)]B_m^{(\mathrm{III})}(k,\omega)}{\varepsilon_2(k,\omega)\frac{K_m'(ka)}{I_m'(ka)} - \varepsilon_1(k,\omega)\frac{K_m(ka)}{I_m(ka)}}, \tag{10c}$$

$$D_m^{(\mathrm{III})}(k,\omega) = [B_m^{(\mathrm{III})}(k,\omega) - K_m(k\rho_0)]\frac{I_m'(kb)}{K_m'(kb)} + C_m^{(\mathrm{III})}(k,\omega). \tag{10d}$$

The DIIMFP is given by

$$\mu^{(\mathrm{III})}(E,\omega) = \frac{-2}{\pi\nu^2}\sum_{m=-\infty}^{\infty}K_m\left(\frac{\omega}{\nu}\rho_0\right)\left\{\mathrm{Im}\left[\frac{D_m^{(\mathrm{III})}\left(\frac{\omega}{\nu},\omega\right)}{\varepsilon_3\left(\frac{\omega}{\nu},\omega\right)}\right] + I_m\left(\frac{\omega}{\nu}\rho_0\right)\mathrm{Im}\left[\frac{1}{\varepsilon_3\left(\frac{\omega}{\nu},\omega\right)}\right]\right\}. \tag{11}$$

D. Limiting cases

Taking $\varepsilon_2=\varepsilon_1$ or $\varepsilon_3=\varepsilon_2$ in Eqs. (6), (9), or (11), one obtains the same formulas of the DIIMFP as those derived in Ref. 12. Taking $\varepsilon_1=\varepsilon_2=\varepsilon_3=\varepsilon$ in Eqs. (6), (9), and (11), one obtains the DIIMFP for an infinite solid as follows:

$$\mu(E,\omega) = \frac{-2}{\pi\nu^2}\sum_{m=-\infty}^{\infty}I_m\left(\frac{\omega}{\nu}\rho_0\right)K_m\left(\frac{\omega}{\nu}\rho_0\right)\mathrm{Im}\left[\frac{1}{\varepsilon\left(\frac{\omega}{\nu},\omega\right)}\right]. \tag{12}$$

Equation (12) may also be found by taking $a\to\infty$ in Eq. (6), $a=0$ and $b\to\infty$ in Eq. (9), or $a=b=0$ in Eq. (11).

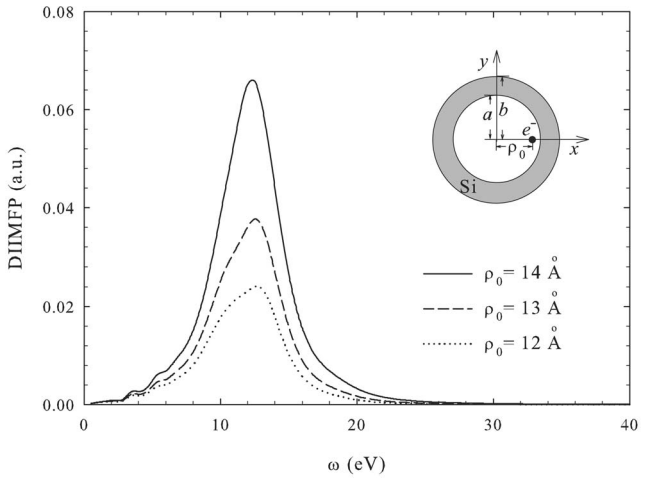

FIG. 2. Calculated DIIMFP for a 500 eV electron moving parallel to and at a distance $\rho_0<15$ Å from the axis of the Si tube of inner radius $a=15$ Å and outer radius $b=25$ Å.

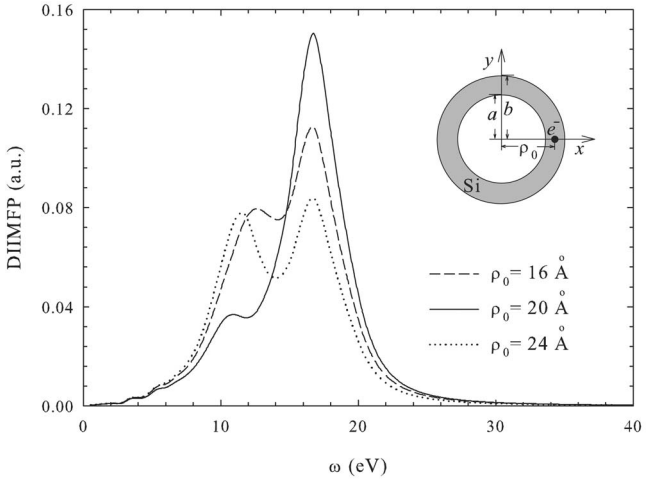

FIG. 3. Calculated DIIMFP for a 500 eV electron moving parallel to and at a distance 15 Å $<\rho_0<$ 25 Å from the axis of the Si tube of inner radius $a=15$ Å and outer radius $b=25$ Å.

III. RESULTS AND DISCUSSION

Using Eqs. (6), (9), and (11), we have calculated the DIIMFP for an electron moving parallel to the axis of a Si cylindrical tube of inner radius $a=15$ Å and outer radius $b=25$ Å. In these calculations, the sum-rule-constrained extended Drude dielectric function with dispersion was applied with parameters determined by a fit[27] of this function to the optical data.[28] Figure 2 shows the results for the DIIMFP of a 500 eV electron traveling inside the Si tube, i.e., $\rho_0<a$, at several distances ρ_0 as a function of energy transfer. It is seen that the DIIMFP is entirely contributed from surface excitations. The surface excitation peak (~12 eV) decreases in magnitude for decreasing ρ_0 due to the weaker response by the solid surface.

The DIIMFP of a 500 eV electron traveling inside the cylindrical shell of the Si tube, i.e., $a<\rho_0<b$, is plotted in Fig. 3 as a function of energy transfer for several values of ρ_0. Since now the electron travels inside the solid, the DIIMFP exhibits overlapping peaks due to the contributions from surface and volume excitations. The relative contributions from surface and volume excitations depend on the location of the electron. As the electron moves along the midline between inner and outer surfaces (solid curve), volume excitations (the peak at ~17 eV) dominate. When the electron moves near the inner surface (dashed curve) or the outer surface (dotted curve), surface excitations (the peak at ~12 eV) become more prominent. In the case of $\rho_0=16$ Å, for instance, the electron moves at 1 Å away from and parallel to the cylindrical surface where the electron and the cylindrical axis are on opposite sides of the surface. In the case of $\rho_0=24$ Å, on the other hand, the electron moves also

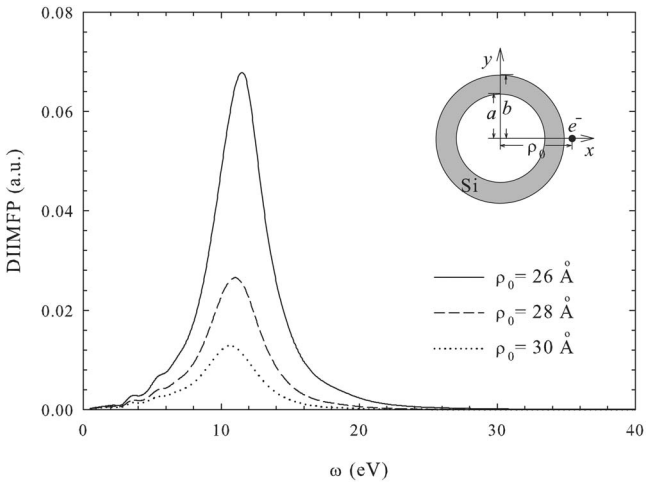

FIG. 4. Calculated DIIMFP for a 500 eV electron moving parallel to and at a distance $\rho_0>25$ Å from the axis of the Si tube of inner radius $a=15$ Å and outer radius $b=25$ Å.

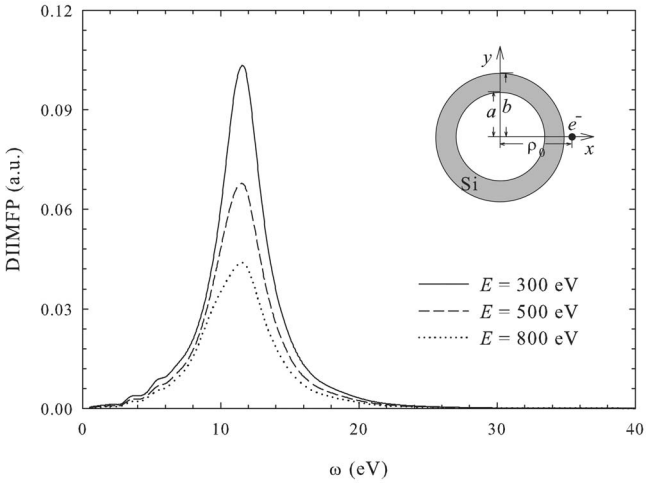

FIG. 5. Calculated DIIMFP for an electron moving parallel to and at a distance $\rho_0=26$ Å from the axis of the Si tube of inner radius $a=15$ Å and outer radius $b=25$ Å for several electron energies.

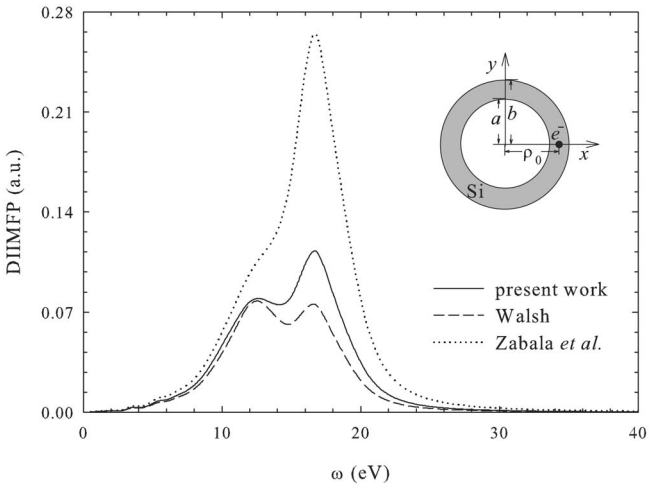

FIG. 6. Calculated DIIMFP for a 500 eV electron moving parallel to and at a distance $\rho_0=16$ Å from the axis of the Si tube of inner radius $a=15$ Å and outer radius $b=25$ Å. Theoretical results calculated using the formulas from Walsh (Ref. 15) and Zabala *et al.* (Ref. 16) based in the same dielectric functions are also plotted for comparisons.

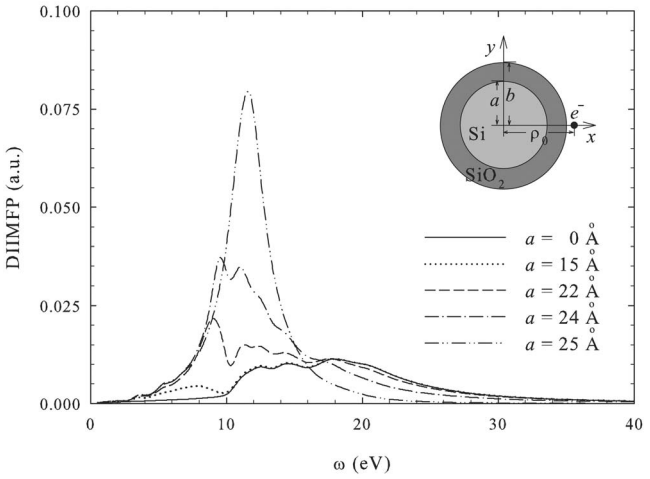

FIG. 7. Calculated DIIMFP for a 500 eV electron moving parallel to and at a distance $\rho_0=26$ Å from the axis of the Si cylinder clad in a SiO2 film, having outer radius $b=25$ Å and inner radius $a=0$, 15, 22, 24 or 25 Å. Results of $a=0$ and 25 Å correspond to the SiO_2 and the Si cylindrical wires.

at 1 Å away from and parallel to the cylindrical surface where the electron and the cylindrical axis are on the same side of the surface. For $\rho_0=16$ Å, the electron moves along the cylindrical surface bending away from it, leading to reduced surface excitations and increased volume excitations. For $\rho_0=24$ Å, the electron moves along the cylindrical surface bending towards it, leading to enhanced surface excitations and decreased volume excitations.

Similar results on the DIIMFP of a 500 eV electron moving outside the Si tube, i.e., $\rho_0>b$, for several ρ_0 are plotted in Fig. 4 as a function of energy transfer. It is seen that in this case the DIIMFP is totally contributed from surface excitations, with its value decreasing for an increasing electron distance from the surface. Figure 5 shows the DIIMFP for electrons with various energies moving outside the Si tube at $\rho_0=26$ Å. It is seen that the DIIMFP decreases with increasing electron energy. This indicates that the contribution from surface excitations also decreases as electron velocity increases.

Figure 6 shows the DIIMFP of a 500 eV electron moving inside the cylindrical shell of the Si tube at $\rho_0=16$ Å. The solid curve represents the results of the present work. Corresponding results of Walsh[15] (dashed curve) and Zabala *et al.*[16] (dotted curve) using the same extended Drude dielectric functions without spatial dispersion are included for comparisons. For electron traveling inside the solid, the DIIMFP contains two peaks corresponding to surface and volume excitations. The peak positions of these excitations in all curves are similar. The peak values of the present work agree reasonably with those of Walsh, but deviate from those of Zabala *et al.* Note that the models of Walsh and Zabala *et al.* were derived with different cutoff momentum transfers and without the consideration of spatial dispersion. Spatial dispersion, however, was considered in the present model.

Figure 7 shows the DIIMFP for a 500 eV electron moving at $\rho_0=26$ Å outside a Si cylinder clad in a SiO_2 film with an outer radius $b=25$ Å and an inner radius $a=15$ Å, 22 Å or 24 Å. For comparisons, corresponding results of a SiO_2 cylindrical wire ($a=0$ Å) and a Si cylindrical wire ($a=25$ Å) are included. In the case of $a=0$ Å, the DIIMFP exhibits a broad distribution contributed from surface excitations of SiO_2. For $a=25$ Å, on the other hand, the DIIMFP is purely contributed from surface excitations of Si. For the Si cylinder clad in a SiO_2 film of thickness 1 Å ($a=24$ Å) or 3 Å ($a=22$ Å), the DIIMFP reveals the contributions from surface (SiO_2-vacuum) excitations and interface (Si-SiO_2) excitations. For the case of a Si cylinder clad in a 10 Å ($a=15$ Å) SiO_2 film, the DIIMFP approaches to that of the SiO_2 cylinder wire. In other words, as the film thickness increases the DIIMFP gradually changes from a value of the Si cylindrical wire to that of the SiO_2 wire. When the film thickness is greater than 10 Å, nearly no contribution from interface excitations is found.

IV. CONCLUSIONS

Based on the dielectric response theory, a theoretical approach was developed to describe the energy loss of an electron moving parallel to the axis of a clad cylindrical system. The DIIMFP of this electron parallel to a Si tube or a Si cylinder clad in a SiO_2 film was calculated using the extended Drude dielectric function with spatial dispersion. It was seen that surface excitations were greater for an electron moving closer to the surfaces of the tube. Volume excitations occurred only for the electron moving inside the solid. It was also seen that the DIIMFP decreased with increasing electron energy. For an electron moving outside a cylinder clad in a film, the DIIMFP was contributed from both surface and interface excitations. The formulas derived in the present work can be applied to any changed particle and any clad cylindrical system of arbitrary materials. However, the present expressions were derived under the assumption of a spatial dispersion parallel to the electron trajectory. A complete treatment including all directions of dispersion is necessary and needs to be further studied.

ACKNOWLEDGMENTS

This research was supported by the National Science Council of the Republic of China under Contract No. NSC94-2215-E-009-080.

[1] R. Núñez, P. M. Echenique, and R. H. Ritchie, J. Phys. C **13**, 4229 (1980).
[2] S. Tougaard and I. Chorkendorff, Phys. Rev. B **35**, 6570 (1987).
[3] S. Tanuma, C. J. Powell, and D. R. Penn, Surf. Interface Anal. **17**, 927 (1991).
[4] A. Jablonski, Prog. Surf. Sci. **79**, 3 (2005).
[5] C. M. Kwei, Y. H. Tu, and C. J. Tung, Nucl. Instrum. Methods Phys. Res. B **230**, 125 (2005).
[6] W. S. M. Werner, Phys. Rev. B **71**, 115415 (2005).
[7] Y. T. Chu, R. J. Warmack, R. H. Ritchie, J. W. Little, R. S. Becker, and T. L. Ferrel, Part. Accel. **16**, 13 (1984).
[8] A. Rivacoba, P. Apell, and N. Zabala, Nucl. Instrum. Methods Phys. Res. B **96**, 465 (1995).
[9] N. Zabala, E. Ogando, A. Rivacoba, and F. J. García de Abajo, Phys. Rev. B **64**, 205410 (2001).
[10] K. Tökési, L. Wirtz, and J. Burgdörfer, Nucl. Instrum. Methods Phys. Res. B **154**, 307 (1999).
[11] K. Tökési and J. Burgdörfer, Surf. Sci. **454-456**, 1038 (2000).
[12] Y. H. Tu, C. M. Kwei, and C. J. Tung, Surf. Sci. **600**, 820 (2006).
[13] N. R. Arista and M. A. Fuentes, Phys. Rev. B **63**, 165401 (2001).
[14] J. L. Gervasoni and N. R. Arista, Phys. Rev. B **68**, 235302 (2003).
[15] C. A. Walsh, Philos. Mag. A **59**, 227 (1989).
[16] N. Zabala, A. Rivacoba, and P. M. Echenique, Surf. Sci. **209**, 465 (1989).
[17] F. J. García de Abajo and P. M. Echenique, Phys. Rev. B **46**, 2663 (1992).
[18] E. Fermi, Phys. Rev. **57**, 485 (1940).
[19] R. H. Ritchie, Phys. Rev. **106**, 874 (1957).
[20] C. M. Kwei, Y. F. Chen, C. J. Tung, and J. P. Wang, Surf. Sci. **293**, 202 (1993).
[21] C. M. Kwei, C. Y. Wang, and C. J. Tung, Surf. Interface Anal. **26**, 682 (1998).
[22] Y. C. Li, Y. H. Tu, C. M. Kwei, and C. J. Tung, Surf. Sci. **589**, 67 (2005).
[23] C. M. Kwei, S. Y. Chiou, and Y. C. Li, J. Appl. Phys. **85**, 8247 (1999).
[24] C. M. Kwei, S. S. Tsai, and C. J. Tung, Surf. Sci. **473**, 50 (2001).
[25] J. D. Jackson, *Classical Electrodynamics* (Wiley, New York, 1975).
[26] F. Yubero, J. M. Sanz, B. Ramskov, and S. Tougaard, Phys. Rev. B **53**, 9719 (1996).
[27] C. M. Kwei, S. J. Hwang, Y. C. Li, and C. J. Tung, J. Appl. Phys. **93**, 9130 (2003).
[28] *Handbook of Optical Constants of Solids*, edited by E. D. Palik (Academic Press, New York, 1985).